THE SPEED CONTROL OF PERMANENT MAGNET SYNCHRONOUS MOTOR USING FUZZY LOGIC AND SELF TUNING FUZZY PI CONTROLLER

Abdulhakim KARAKAYA
e-mail: akarakaya@kou.edu.tr

Ercüment KARAKAŞ
e-mail: karakas@kou.edu.tr

Department of Electrical Education, University of Kocaeli, Izmit 41380, Kocaeli, Turkey.
Keywords: Permanent Magnet Synchronous Motor, F and STFLPI.

ABSTRACT

This paper obtains a nonlinear mathematical model of PMSM, and realizes simulation of obtained model in Matlab/Simulink program. Speed control of motor model is made with Fuzzy Logic (FL) and Self Tuning FLPI (STFLPI) controllers. Controller performances are compared from the speed graphs obtained.

I. INTRODUCTION

In high performance applications, the Permanent Magnet Synchronous Motors (PMSMs) are becoming popular as compared to other types of ac motor due to some of their advantageous features including high torque, high power, high efficiency and low noise. Insensitivity to parameter variation and, reaching of the speed to a reference value at shortest time due to any disturbances, are some of the important criteria of the high performance drive systems used for drive PMSMs in robotics, rolling mills, machine tolls etc. The conventional proportional integral (PI) and proportional integral derivative (PID) controllers have been widely utilized as speed controllers in PMSM drives. However in order to obtain the best results from the controls, the d-q axis reactance parameters of the PMSM must be known exactly. This is rather difficult and conventional fixed gain PI and PID controllers are very sensitive to step change of command speed, parameter variations and load disturbance [1]. Therefore, a special controller of PMSM is needed to make speed control in high performance drive systems [2].

In the literature on PMSM, it is seen that; Güney et al [3] examined dynamic behaviour model of permanent magnet synchronous motor using PWM inverter and fuzzy logic controller for stator phase current, flux and torque control of PMSM. Ohm et al [4], established a mathematical model of PMSM and obtained parameters of PMSM experimentally. Singh et al [5] examined current, voltage, speed and torque variation graphs and realized performance analysis with FL controller of PMSM driver. Uddin and Rahman [2] compared simulation results with responses obtained from experiments and made FL fundamental speed control of Interior PMSM. Senjyu et al [6] worked on measurement of real parameters for high speed PMSMs and made comparison between calculated values and measured values.

This paper obtains mathematical model of PMSM, realizes simulation of the model obtained in Matlab/Simulink program. The parameters used in simulation, are the real measured values from PMSM of 260.75 W power, and from motor speed graphs obtained with these parameters, rise time, settling time, overshoot and steady-state error analyses are made. In the speed control block in Fig. 1 Proportional Integral (PI), Fuzzy Logic (FL), Fuzzy Logic PI (FLPI) and Self Tuning FLPI (STFLPI) controllers are used and performances of controllers are compared. Necessary parameters are shown in Table 9.
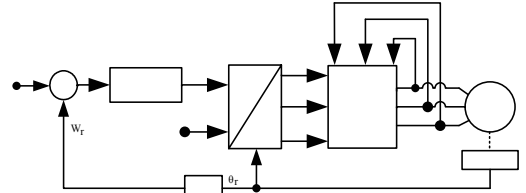
Fig. 1. Speed control block diagram of PMSM.

II. MATHEMATICAL MODEL OF PMSM.

Fig. 1 shows speed control block diagram of PMSM. The PMSM is fed by a current-controlled pulse width modulated (PWM) inverter. The motor currents are decomposed into i_d and i_q components which are respectively flux and torque components in the rotor-based d-q coordinates system [7]. Motor model is constituted with following equations:

$$T_e = \frac{3}{2}\frac{P}{2}\left[\lambda_m.i_q + \left(L_d - L_q\right)i_d.i_q\right] \qquad (1)$$

$$\frac{d(i_d)}{dt} = \frac{v_d - r_s.i_d + w_r.L_q.i_q}{L_d} \qquad (2)$$

$$\frac{d(i_q)}{dt} = \frac{v_q - r_s.i_q - w_r.(L_d.i_d + \lambda_m)}{L_q} \qquad (3)$$

$$\frac{d(w_{rm})}{dt} = \frac{T_e - T_L - B.w_{rm}}{J} \qquad (4)$$

$$w_r = \frac{P}{2}.w_{rm} \qquad (5)$$

Where T_L is the load torque, B is the viscous friction, J is the moment of inertia, V_d and V_q represent the d-q axes stator voltages, i_d and i_q are the d-q axis stator currents. L_d and L_q are the d-q axis inductances, r_s is the per phase stator resistance, w_r shows the electrical velocity of the rotor. λ_m is expression of the flux linkage due to the rotor magnets linking the stator, T_e is the motor produced torque and w_{rm} is the mechanical velocity of the rotor.

III. FUZZY LOGIC CONTROLLER

If structure of FL controller is investigated as shown in Fig. 2 (a), controller has two input variables; speed error e(k) and change of speed error ce(k) [9]. At the same time, change in reference phase current $i_q^*(k)$ is output $\Delta i_q^*(k)$.

(a)

(b)
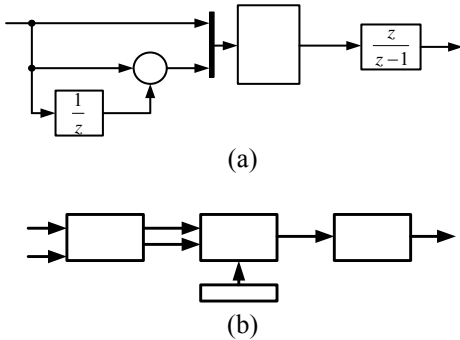
Fig. 2. (a) Structure of FL controller. **(b)** FL controller internal structure.

e(k) and ce(k) are calculated as in equations (24) and (25) for every sampling time:

$$e(k) = w^*(k)-w_r(k) \qquad (6)$$
$$ce(k) = e(k)-e(k-1) \qquad (7)$$

Where $w^*(k)$ is reference speed and $w_r(k)$ is actual speed value.

In the first stage, the crisp variables e(k) and ce(k) are converted into fuzzy variables e and ce using the triangular membership functions shown in Fig. 3. The universes of discourse of the input variables e and ce are respectively (-110, 110) rad/s and (-0.89, 0.89) rad/s. The universe of discourse of the output variable Δi_q^* is (-1, 1) A. Each universe of discourse is divided into seven fuzzy

sets: Negative Big (NB), Negative Medium (NM), Negative Small (NS), Zero (Z), Positive Small (PS), Positive Medium (PM) and Positive Big (PB).
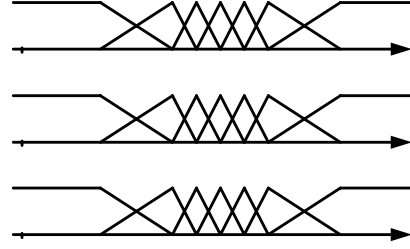
Fig. 3. Membership functions of the fuzzy variables e, ce and Δi_q^*.

In the second stage, the FL controller executes the 49 control rules shown in Table 1 taking the fuzzy variables e and ce as inputs and the output quantity Δi_q^* is processed in the defuzzification unit. The rules are formulated using the knowledge of the PM synchronous motor behavior and the experience of control engineers.

Table 1. Fuzzy control rules for speed controller.

		Error "e"						
		NB	NS	NS	Z	PS	PM	PB
Change of error "ce"	NB	NB	NB	NB	NB	NM	NS	Z
	NM	NB	NB	NB	NM	NS	Z	PS
	NS	NB	NB	NM	NS	Z	PS	PM
	Z	NB	NM	NS	Z	PS	PM	PB
	PS	NM	NS	Z	PS	PM	PB	PB
	PM	NS	Z	PS	PM	PB	PB	PB
	PB	Z	PS	PM	PB	PB	PB	PB

As shown in Fig. 2 (b), the inference engine output variable Δi_q^* is converted into a crisp value $\Delta i_q^*(k)$ in the defuzzification unit. Various defuzzification algorithms have been proposed in the literature [8]. Here, the centroid defuzzification algorithm is used in which the crisp value is calculated as the center of gravity of the membership function of Δi_q^* as in equation (8):

$$\Delta i_q^*(k) = \frac{\sum_{i=1}^{n} (\Delta i_q^*)_i \, \mu[(\Delta i_q^*)_i]}{\sum_{i=1}^{n} \mu[(\Delta i_q^*)_i]} \qquad (8)$$

The reference current $i_q^*(k)$ for the vector control system is obtained by integrating $\Delta i_q^*(k)$ as in equation (9):

$$i_q^*(k) = i_q^*(k-1) + \Delta i_q^*(k) \qquad (9)$$

IV. SELF TUNING FUZZY PI CONTROLLER

Block diagram of STFLPI controller is shown in Fig. 4. Output of FL controller is improved by self tuning mechanism. The necessary background for this mechanism is given in the following subsection.
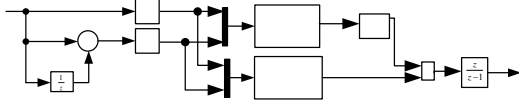
Fig. 4. Block diagram of STFLPI controller.

A. Membership functions

Input membership functions e(k) and ce(k) are (-1, 1) rad/s and output membership function $\Delta i_q(k)$ is (-1, 1) A. At the same time, the scaling factor for self tuning mechanism inputs (E(k), CE(k)) and α are used as (0, 1). For input and output variables, necessary rule bases are shown in Table 1 and membership functions in Fig. 5. Membership functions are shown for self tuning mechanism block in Fig. 6. For determination of gain updating factor α (7x7) control rules (Zero (Z), Very Small (VS), Small (S), Small Big (SB), Medium Big (MB), Big (B), Very Big (VB)) as shown in Table 2 and triangle membership functions shown in Fig. 10, are used.
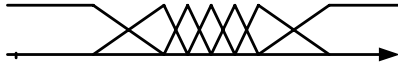
Fig. 5. Memberships functions for E, CE and ΔI_q

B. Scaling factors

The relationships between the scaling factors (G_e, G_{ce} and $G_{\Delta Iq}$) of input and output variables of the STFLPI are as in equations (10), (11) and (12):

$$E(k) = e(k).G_e(k) \tag{10}$$

$$CE(k) = ce(k).G_{ce}(k) \tag{11}$$

$$\Delta i_q^*(k) = \alpha.\Delta I_q(k).G_{\Delta I_q}(k) \tag{12}$$

In equation (12), α is the gain updating factor. Unlike FLPI controller (which uses only $G_{\Delta Iq}$) the actual output ($\Delta i_q^*(k)$) for STFLPI controller is obtained using the effective scaling factor ($\alpha.G_{\Delta Iq}$) as shown in Fig. 4. Suitable values for G_e, G_{ce} and $G_{\Delta Iq}$ are respectively determined to be 0.0091, 1 and 0.5.

C. The rule-bases

Rules of FLPI controller is shown in Table 1. The gain updating factor (α) is calculated using fuzzy rules. Rule base in Table 2 is used for calculation of α.

Table 2. Fuzzy rules for calculation of α.

		Error "e"						
		VB	B	MB	SB	S	VS	Z
Change of error "ce"	VB	VB	VB	VB	B	SB	S	Z
	B	VB	VB	B	B	MB	S	VS
	MB	VB	MB	B	VB	VS	S	VS
	SB	S	SB	MB	Z	MB	SB	S
	S	VS	S	VS	VB	B	MB	VB
	VS	VS	S	MB	B	B	VB	VB
	Z	Z	S	SB	B	VB	VB	VB

V. COMPARATIVE STUDY OF SPEED RESPONSES

A. No-load condition

System is run, while motor shaft is under no load condition. While reference speed is 100 rad/s, graphs obtained are shown in Fig. 7. In Table 3, t_{ro} is the rise time of angular speed, t_{so} is settling time of angular speed, O_s is the overshoot and e_{ss} is the steady-state error and shown result to obtained from controllers.
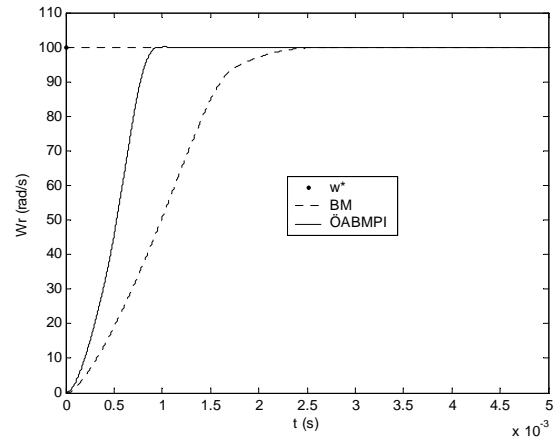
Fig. 7. Speed responses of PMSM under no load obtained with FL and STFLPI controllers.

Table 3. While PMSM is under no load, speed performance analyses of FL and STFLPI controllers.

Controller	t_{ro} (s)	t_{so} (s)	O_s (%)	e_{ss}
FL	0.002832	0.0036	0.0131	0.0028
STFLPI	0.000990	0.0013	0.0487	0.0055

Table 4. While PMSM is under no load, comparison of controller performances.

Controllers	t_{ro} (%)	Controllers	t_{so} (%)
STFLPI -FL	48	STFLPI -FL	46
Controllers	**O_s (%)**	**Controllers**	**e_{ss} (%)**
FL- STFLPI	58	FL- STFLPI	32

In Table 4, controllers are compared among themselves in percentages. It is seen that in rise time of angular speed and in settling time of the angular speed the STFLPI, but

in overshoot and in steady-state error the FL, exhibit the best performance.

B. Load condition

System is run, while motor shaft is under load condition. Graphs obtained are shown in Fig. 8 while reference speed is 100 rad/s. In Table 5, t_{rL} is the rise time of the angular speed and t_{sL} is the settling time of the angular speed both under load condition. Also shown are results obtained from controllers.
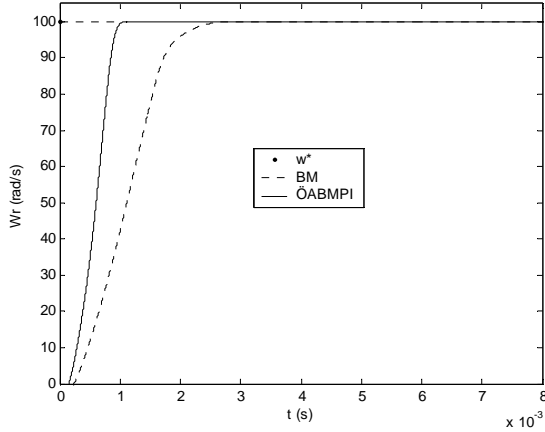
Fig. 8. Speed responses of PMSM under load obtained with FL and STFLPI controllers.

Table 5. While PMSM is under load, speed performance analyses of FL and STFLPI controllers.

Controller	t_{rL} (s)	t_{sL} (s)	O_s (%)	e_{ss}
FL	0.002907	0.0036	0.0178	0.0027
STFLPI	0.001070	0.0014	0.0893	0.0054

Table 6. While PMSM is under load, comparison of controller performances.

Controllers	t_{rL} (%)	Controllers	t_{sL} (%)
STFLPI -FL	46	STFLPI -FL	44
Controllers	O_s (%)	**Controllers**	e_{ss} (%)
FL- STFLPI	66	FL- STFLPI	34

In Table 6, controllers are compared among themselves in percentages. It is seen that in rise and settling times of angular speed STFLPI and in overshoot and steady-state error the FL controllers exhibit the best performance.

C. Step load torque application

After motor makes no-load departure, step load torque of nominal load (0.83 Nm) is applied to the system at 0.04 s. While reference speed is 100 rad/s, graphs obtained are shown in Fig. 9. In Table 7, Δt_i is the settling time, Δw_i is the angular speed change, O_{si} is the overshoot, and e_{ssi} is the steady-state error of the motor, all of which are determined under a step load of nominal value.
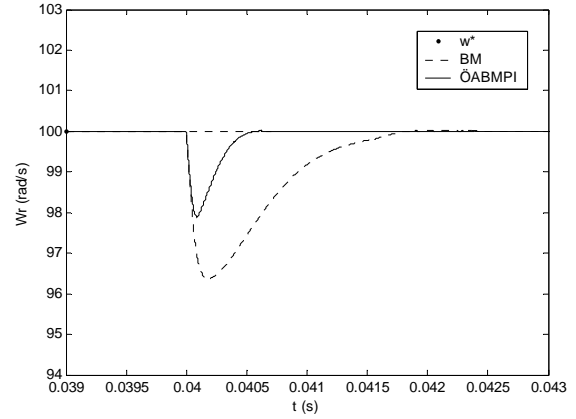
Fig. 9. Speed response to step load torque application with FL and STFLPI controllers.

Table 7. While PMSM is under step load, speed performance analyses of FL and STFLPI controllers.

Controller	Δt_i (s)	Δw_i (%)	O_{si} (%)	e_{ssi}
FL	0.0060	3.65570	0.0290	0.0028
STFLPI	0.0006	2.11230	0.0122	0.0053

Table 8. While PMSM is under step load, comparison of controller performances.

Controllers	Δt_i (s)	Controllers	Δw_i (%)
STFLPI -FL	82	STFLPI -FL	26
Controllers	O_{si} (%)	**Controllers**	e_{ssi} (%)
STFLPI -FL	40	FL- STFLPI	30

In Table 8, controllers are compared among themselves in percentages. It is seen that in settling time and angular speed change, in overshoot the STFLPI, and in steady-state error the FL controllers exhibit the best performance.

VI. CONCLUSION

In this paper, different controllers for PMSM are used and the following results are obtained in the speed control;

STFLPI controller gives the best performance in settling time under no load, load and step load conditions. Inspection of Tables 4, 6 and 8 reveals that under no load condition, in settling time STFLPI controller is 46% better than FL controller. Under load condition in settling time, STFLPI controller is 44% better than FL controller. Under step load, STFLPI controller is 82% better than FL controller. From an observation of these percentages one can see that superiority of STFLPI in settling time is most marked under step load condition.

In general it can be concluded that in practices with step load application use of STFLPI controller, and in those with small steady-state error requirement use of FL controller is best for the given system.

Table 9. Parameters of PMSM.

V (V)	530
f (Hz)	50
P	6
r_s (Ω)	5.25
L_d (mH)	11.83
L_q (mH)	13.33
λ_m (Wb)	0.09653
B (Nm/(rad/s))	0.00014324
J (kgm^2)	0.000054
T_L (Nm)	0.83

KAYNAKLAR

1. Rahman, M. A., Hoque, M. A., 1997. On-line self-tuning ANN based speed control of a PM DC motor. IEEE/ASME Trans. On Mechatronics 2 (3), pp.169-178.

2. Uddin, M. N., Rahman M. A., 2000. Fuzzy logic based speed control of an IPM synchronous motor drive. Journal of Advanced Computational Intelligence 4 (2), pp. 212-219.

3. Güney, İ., Yüksel, O., Serteller, F., 2001. Dynamic behaviour model of permanent magnet synchronous motor fed by PWM inverter and fuzzy logic controller for stator phase current, flux and torque control of PMSM. International Electric Machines and Drive Conference, pp. 479-485.

4. Ohm, D.Y., Brown, J. W., Chava, V.B., 1995. Modeling and parameter characterization of permanent magnet synchronous motor. Proceeding of the 24th Annual Symposium of Incremental Motion Control Systems and Devices, Sn Jose, pp. 81-86.

5. Singh, B., Putta Swamy, C.L., Singh, B.P., Chandra, A., Al-Haddad, K., 1995. Performance analysis of fuzzy logic controlled permanent magnet synchronous motor drive. Proceedings of IEEE-ICON l (1), 399-405.

6. Senjyu, T., Kuwae Y., Urasaki N., Uezato K., 2001. Accurate parameter measurement for high speed permanent magnet synchronous motors. Power Electronics Specialists Conference 2, pp. 772-777.

7. Krause, P.C., 1987. Analysis of electric machinery. McGraw-Hill, New York.

8. Sousa, G.C.D., Bose, B.K., 1991. A fuzzy set theory based control of a phase-controlled converter dc machine drive. Industry Applications Society Annual Meeting Conference Record, pp. 854-861.

9. Yager, R. R., Filev, D. P., "Essentials of fuzzy modeling and control", John Wiley & Sons Inc., Canada, 1994.